

Polymer Chemistry

Volume 17
Number 12
24 March 2026
Pages 1135-1234

rsc.li/polymers



ISSN 1759-9962

PAPER

Takahiro Iwamoto *et al.*
Synthesis of network polymers composed of well-defined
silyl ether macrocycles



Fig. 1 The synthetic strategy for silyl ether-based network polymer consisting of well-defined macrocyclic structures.

diol (**3**) as a linker (Scheme 1). Following the previously reported method, dichlorosilacyclobutane was treated with dihydroxybiphenyl in the presence of imidazole. The reaction afforded the desired product along with small amount of byproduct. After washing the crude product by acetonitrile, an analytically pure macrocycle was obtained in 90% yield. ^1H , ^{13}C , and ^{29}Si NMR spectroscopic analyses and mass spectrometry supported the formation of macrocycle **2** with exclusive selectivity. A rapid and efficient synthesis was also achieved when used with diol **3**. In this case, the starting diol was hardly dissolved in THF, while the reaction efficiently proceeded to provide soluble macrocyclic compound **4** almost



Scheme 1 Macrocyclizations of diols with dichlorosilacyclobutane to provide macrocycles **2** and **4**.

quantitatively. The structure was further examined by single-crystal X-ray diffraction. Although the crystal quality was insufficient for full structural refinement (see SI), the analysis indicated that macrocycle **4** consists of four silacyclobutane units and four bicyclohexylene linkers, adopting an approximately square-shaped geometry in the solid state. This structural motif closely resembles that of the macrocycles reported in our previous work, whereas the conformations of the silyl ether units show slight variations that reflect their inherent flexibility.

Polymerization *via* the ring-opening reaction of the silacyclobutane units was first assessed by thermogravimetric analyses (TGA) and differential scanning calorimetry (DSC). As shown in Fig. 2a, macrocycle **2** exhibited melting point at 168 °C and subsequently an exothermic peak ranging from 217 °C to 338 °C. The exothermic peak was no longer observed upon reheating the sample. After heating over the observed exothermic peak, the sample became insoluble in common organic solvents. Fourier transform infrared (FTIR) spectroscopy indicated that, upon heating, a characteristic peak at 1121 cm^{-1} assigned to the silacyclobutane ring significantly decreased.¹⁷ These observations implied that a polymeric structure was formed *via* ring-opening reaction of the silacyclobutane units. We have already reported that macrocycle **5** bearing Me_2Si units instead of silacyclobutane unit at the vertices exhibited high thermal stability within 300 °C (Fig. 3). Furthermore, the peak of the reference compound **5** at around the characteristic peak of the silacyclobutane unit in the FT-IR spectrum remained essentially unchanged (see the SI). On the basis of these results, we concluded that the macrocyclic skeleton is maintained during the ring-opening reaction of the silacyclobutane unit. Note that other peaks particularly derived from linker units hardly changed upon the ring-opening reaction. This result also supported retention of the macrocyclic skeleton during the ring-opening reaction. Macrocycle **4** showed a similar thermal response (Fig. 2b). Although the



Fig. 2 DSC analyses and FT-IR spectra of macrocycle **2** (a) and **4** (b). FT-IR analyses were performed by using the samples used in TGA analyses.



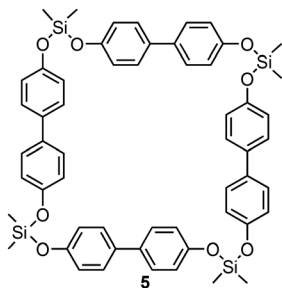


Fig. 3 Structure of macrocycles 5.

exothermic enthalpy derived from the ring-opening reaction was slightly lower than that of macrocycle 2, FT-IR analysis of the obtained sample indicated that efficient consumption of the silacyclobutane units. Therefore, we concluded that a polymer network is formed also in a reaction of macrocycle 4.

Next, we investigated the effect of heating conditions on network formation (Fig. 4). Macrocycle 2 bearing biphenylene linkers was used for this study. When the sample was continuously heated at $10\text{ }^{\circ}\text{C min}^{-1}$ up to $350\text{ }^{\circ}\text{C}$ (condition A, red line in Fig. 4a), the resulting material was visually transparent. Strong birefringence was observed under polarized optical microscopy (POM) (Fig. 4b). Although birefringence suggests the presence of molecular orientation, no diffraction peaks were detected in the XRD analysis, indicating that the degree of orientation was limited and did not lead to long-range



Fig. 4 (a) Examination of heating conditions of the ring-opening reactions of macrocycle 2. (b) Appearance, POM, and SEM images of the samples obtained by DSC under conditions A–C.

order. In contrast, when the sample was held isothermally at its melting point for 15 minutes (condition B, black line), the birefringence became significantly weaker. These observations suggest that rapid heating promotes network formation while partially retaining the molecular orientation inherited from the crystalline initial material, whereas isothermal annealing at the melting point relaxes these orientations prior to network formation.

We next examined holding the sample at the melting point for 3 hours before the thermal polymerization (condition C, blue line). In this case, a distinct behavior was observed: a new endothermic peak appeared at $205\text{ }^{\circ}\text{C}$, different from the ring-opening process. After the subsequent heating for the thermal polymerization, exothermic peak derived from the ring-opening was observed. The cured material appeared turbid, and SEM imaging revealed the presence of particles with diameters of approximately $1.7\text{ }\mu\text{m}$. Notably, such particles were absent in the materials obtained under conditions A and B. We have previously shown that a similar type of macrocyclic molecule can exhibit cold crystallization.²⁷ Thus, we assumed that the newly observed endothermic peak should be attributed to the melting of crystals formed by cold crystallization during the holding for 3 h at $160\text{ }^{\circ}\text{C}$. Overall, these results demonstrate that the heating protocol strongly influences not only the orientation of the macrocyclic units but also the bulk morphology of the resulting polymer network.

With these results in mind, we next prepared thin films *via* drop-casting a solution of macrocycle 2 onto a glass substrate, followed by heating at $255\text{ }^{\circ}\text{C}$ for 1 h (film A). The treatment temperature of $255\text{ }^{\circ}\text{C}$ was chosen because it lies within the exothermic region associated with the ring-opening of the silacyclobutane units, allowing efficient network formation under melt conditions. The resulting film became insoluble in common organic solvent. Additionally, FT-IR spectrum was identical to that obtained after DSC analysis (see the SI), confirming successful polymerization. SEM images revealed smooth surfaces, and powder X-ray diffraction showed no distinct diffraction peaks, indicating that the films were amorphous. The transparent appearance and the negligible birefringence observed under POM suggested that the obtained films closely resembled those produced under condition B in Fig. 4a. The same procedure was applied to the preparation of thin film of macrocycle 4 (film B). The obtained film was insoluble and exhibited IR spectra consistent with those of the sample obtained by DSC. The films were also optically transparent, transmitting more than 97% of visible light. In both cases, the high optical transmittance is consistent with the absence of crystal aggregation, as supported by the XRD and SEM analyses (Fig. 5).

The thermal stability of the resulting films was evaluated by TGA under a nitrogen atmosphere. For both films A and B, no 5% weight loss (T_{d5}) was observed below 517 and $481\text{ }^{\circ}\text{C}$, respectively, demonstrating their high thermal resistance (Fig. 6a). In contrast, the macrocyclic monomer 5 decomposed at approximately $350\text{ }^{\circ}\text{C}$ ($T_{d5} = 367\text{ }^{\circ}\text{C}$). Therefore, the excellent heat resistance of the films originates not only from the





Fig. 5 Appearance, SEM images, and UV-vis absorption spectra of the films obtained by thermal treatment of macrocycle 2 (a) and 4 (b).



Fig. 6 (a) TGA thermograms, (b) elastic modulus and instrumented indentation hardness, and (c) water contact angles of film A and B.

inherent stability of the silyl ether units but also from the formation of a high cross-linking network structure.

The mechanical properties of the films were assessed by nanoindentation using a Shimadzu DUH-211 device equipped with a Triangular115 indenter (Fig. 6b). Despite the presence of a highly crosslinked network, the films exhibited relatively low hardness (190 MPa) and a modest elastic modulus (2023 MPa). This mechanically soft behavior is attributed to the flexibility of the silyl ether units within the network. A similar mechanical profile was observed for film B. Interestingly, films derived from macrocycle 4 displayed even lower mechanical rigidity, highlighting the impact of the linker structure on the mechanical properties of the resulting networks.

Although macrocycles 2, 4, and 5 are highly susceptible to hydrolysis in their isolated state, the corresponding films exhibited markedly enhanced resistance toward hydrolysis even under acidic conditions. After immersion in ethanol containing 1 M HCl for 24 h, the films showed a 34% weight loss (see SI for details). A ¹H NMR spectrum of the soluble fraction

obtained after acidic treatment indicated the film was decomposed to the corresponding diol species (see the SI). While the extent of decomposition was not negligible, this result clearly indicates a substantial increase in hydrolytic stability, as macrocycles 2 and 4 readily decompose under ambient conditions. A similar trend was observed for film B. In both films, the network structure remains largely preserved under neutral conditions. This enhanced durability is likely attributable to the dense cross-linked network and/or the hydrophobic surface, which may limit the accessibility of water and acid to the hydrolyzable silyl ether bonds. To assess the surface properties of the films, static water contact angle measurements were conducted (Fig. 6c). The measured contact angle for film A was $95.1 \pm 0.2^\circ$, indicating an intrinsically hydrophobic surface. Film B also exhibited hydrophilic surface with water contact angle of $86.3 \pm 0.5^\circ$. Interestingly, despite its more hydrophobic linker structure, film B displayed a lower contact angle than film A. This apparent discrepancy may arise from microscopic differences in surface topography. Gas sorption measurements showed negligible N₂ and CO₂ uptake, indicating the absence of permanent microporosity in the network structure (see SI). These structures might also inhibit access of water to the hydrolyzable silyl ether bonds.

Conclusions

In summary, we have demonstrated a facile synthetic route to silyl ether-based network polymers through efficient macrocyclization of diols with dichlorosilacyclobutane, followed by thermal ring-opening of the silacyclobutane units. This strategy enabled the direct incorporation of well-defined macrocyclic motifs into a polymer backbone, a structural feature rarely explored in conventional silyl ether polymer chemistry. The resulting crosslinked networks exhibited excellent thermal stability and optical transparency, together with remarkable resistance to hydrolytic degradation despite the intrinsic sensitivity of the macrocyclic precursors. Mechanical tests further revealed that the inherent flexibility of the silyl ether linkages imparts relatively low hardness and modulus, while the linker structure significantly influences the final material properties. Incorporating well-defined macrocyclic motifs into a polymer skeleton could unlock unexplored opportunities to design a novel silyl ether-based polymer. Thus, investigation of other diol structures is currently underway.

Conflicts of interest

There are no conflicts to declare.

Data availability

The data supporting this article have been included as part of the supplementary information (SI). Supplementary



information is available. See DOI: <https://doi.org/10.1039/d6py00035e>.

Acknowledgements

This work was supported by the Izumi Science and Technology Foundation, Proterial Materials Science Foundation, Shorai Foundation for Science and Technology, and Ogasawara Foundation for the Promotion of Science and Engineering. Diol 3 was kindly gifted by JNC.

References

- 1 E. Yilgör and I. Yilgör, *Prog. Polym. Sci.*, 2013, **39**, 1165–1195.
- 2 S. Gao, Y. Liu, S. Feng and Z. Lu, *J. Mater. Chem. A*, 2019, **7**, 17498–17504.
- 3 Y. Zhang, Z. Zhu, Z. Bai, W. Jiang, F. Liu and J. Tang, *RSC Adv.*, 2017, **7**, 16616–16622.
- 4 X. Chen, L. Fang, X. Chen, J. Zhou, J. Wang, J. Sun and Q. Fang, *ACS Sustainable Chem. Eng.*, 2018, **6**, 13518–13523.
- 5 C. M. Bunton, Z. M. Bassampour, J. M. Boothby, A. N. Smith, J. V. Rose, D. M. Nguyen, T. H. Ware, K. G. Csaky, A. R. Lippert, N. V. Tsarevsky and D. Y. Son, *Macromolecules*, 2020, **53**, 9890–9900.
- 6 C. Cheng, A. Watts, M. A. Hillmyer and J. F. Hartwig, *Angew. Chem., Int. Ed.*, 2016, **55**, 11872–11876.
- 7 S. Vijjamarri, M. Hull, E. Kolodka and G. Du, *ChemSusChem*, 2018, **11**, 2881–2888.
- 8 H. Fouilloux, M.-N. Rager, P. Ríos, S. Conejero and C. M. Thomas, *Angew. Chem., Int. Ed.*, 2022, **61**, e202113443.
- 9 M. C. Parrott, J. C. Luft, J. D. Byrne, J. H. Fain, M. E. Napier and J. M. DeSimone, *J. Am. Chem. Soc.*, 2010, **132**, 17928–17932.
- 10 P. Zheng and T. J. McCarthy, *J. Am. Chem. Soc.*, 2012, **134**, 2024–2027.
- 11 W. Schmolke, N. Perner and S. Seiffert, *Macromolecules*, 2015, **48**, 8781–8788.
- 12 T. Debsharma, V. Amfilochiou, A. A. Wróblewska, I. D. Baere, W. V. Paepegem and F. E. D. Prez, *J. Am. Chem. Soc.*, 2022, **144**, 12280–12289.
- 13 K. E. L. Husted, C. M. Brown, P. Shieh, I. Kevlishvili, S. L. Kristufek, H. Zafar, J. V. Accardo, J. C. Cooper, R. S. Klausen, H. J. Kulik, J. S. Moore, N. R. Sottos, J. A. Kalow and J. A. Johnson, *J. Am. Chem. Soc.*, 2023, **145**, 1916–1923.
- 14 R. MacFarlane and E. S. Yankura, *Synthesis of Regulated Structure Polyphenylether Siloxane Block Copolymers*, United States Rubber Co Naugatuck CT Chemical Div., 1963.
- 15 J. E. Curry and J. D. Byrd, *J. Appl. Polym. Sci.*, 1965, **9**, 295–311.
- 16 S. Luleburgaz, U. Tunca and H. Durmaz, *Polym. Chem.*, 2023, **14**, 2949–2957.
- 17 W. Yuan, X. Wei, Q. Peng, L. Fan, X. Li, H. Hu, Y. Huang, J. Ma and J. Yang, *J. Appl. Polym. Sci.*, 2021, **138**, e51376.
- 18 X. Wu, O. Grinevich and D. C. Neckers, *Chem. Mater.*, 1999, **11**, 3687–3692.
- 19 G. Raabe and J. Michl, *Chem. Rev.*, 1985, **85**, 419–509.
- 20 H. Yamashita, M. Tanaka and K. Honda, *J. Am. Chem. Soc.*, 1995, **117**, 8873–8874.
- 21 R. Jain, A. P. J. Brunskill, J. B. Sheridan and R. A. Lalancette, *J. Organomet. Chem.*, 2005, **690**, 2272–2277.
- 22 K. Matsumoto and H. Yamaoka, *Macromolecules*, 1995, **28**, 7029–7031.
- 23 T. Iwamoto, S. Amano, K. Maeda, N. Shibama, W. Sekiguchi, Y. Kazama, Y. Nakamura, K. Sugamata, H. Imoto, K. Naka and Y. Ishii, *Chem. Commun.*, 2025, **61**, 8180–8183.
- 24 F. Garnes-Portolés and A. Leyva-Pérez, *ACS Catal.*, 2023, **13**, 9415–9426.
- 25 V. Martí-Centelles, M. D. Pandey, M. I. Burguete and S. V. Luis, *Chem. Rev.*, 2015, **115**, 8736–8834.
- 26 J. Blankenstein and J. Zhu, *Eur. J. Org. Chem.*, 2005, 1949–1964.
- 27 T. Iwamoto, S. Amano, K. Maeda, N. Shibama, W. Sekiguchi, A. Imaizumi, A. Honda, H.-C. Chang, H. Houjou, H. Imoto, K. Naka and Y. Ishii, *J. Phys. Chem. B*, 2026, **130**, 1724–1729.

